

Discovery of hot subdwarfs covered with helium-burning ash

Klaus Werner,^{1*} Nicole Reindl,² Stephan Geier² and Max Pritzkeleit²

¹*Institut für Astronomie und Astrophysik, Kepler Center for Astro and Particle Physics, Universität Tübingen, Sand 1, 72076 Tübingen, Germany*

²*Institut für Physik und Astronomie, Universität Potsdam, Karl-Liebknecht-Straße 24/25, 14476, Potsdam, Germany*

February 14, 2022

ABSTRACT

Helium rich subdwarf O stars (sdOs) are hot compact stars in a pre-white dwarf evolutionary state. Most of them have effective temperatures and surface gravities in the range $T_{\text{eff}} = 40\,000\text{--}50\,000\text{ K}$ and $\log g = 5.5\text{--}6.0$. Their atmospheres are helium dominated. If present at all, C, N, and O are trace elements. The abundance patterns are explained in terms of nucleosynthesis during single star evolution (late helium core flash) or a binary He-core white dwarf merger. Here we announce the discovery of two hot hydrogen-deficient sdOs (PG1654+322 and PG1528+025) that exhibit unusually strong carbon and oxygen lines. A non-LTE model atmosphere analysis of spectra obtained with the Large Binocular Telescope and by the LAMOST survey reveals astonishingly high abundances of C ($\approx 20\%$) and O ($\approx 20\%$) and that the two stars are located close to the helium main sequence. Both establish a new spectroscopic class of hot H-deficient subdwarfs (CO-sdO) and can be identified as the remnants of a He-core white dwarf that accreted matter of a merging low-mass CO-core white dwarf. We conclude that the CO-sdOs represent an alternative evolutionary channel creating PG1159 stars besides the evolution of single stars that experience a late helium-shell flash.

Key words: stars: abundances – stars: atmospheres – stars: evolution – subdwarfs

1 INTRODUCTION

In the Kiel diagram, helium rich subdwarf O stars (He-sdOs) cluster around effective temperatures and gravities of $T_{\text{eff}} = 40\,000\text{--}50\,000\text{ K}$ and $\log g = 5.5\text{--}6.0$ (Heber 2016). They exhibit little or no hydrogen in their atmospheres. The carbon abundance is either slightly above the solar value (up to about $C = 0.03$ mass fraction) or strongly depleted. Nitrogen is 3–10 times oversolar for many He-sdOs while it is strongly depleted in others. Abundance measurements of oxygen are scarce and reveal values (strongly) below the solar abundance, see e.g. Schindewolf et al. (2018) and Werner et al. (2021). The abundance patterns indicate the dominance of hydrogen-burning ash on the stellar surface. As to the origin of He-sdOs, two competing scenarios are discussed, namely a late He-core flash (e.g. Battich et al. 2018) or a He-core white dwarf merger (Zhang & Jeffery 2012). The He-sdOs are on or near the helium main sequence and evolutionary models suggest that they are either He-core or He-shell burners, respectively.

In contrast to all He-sdOs studied so far, we present here two exceptional objects of a new spectral class that we call CO-sdOs. They caught our attention because they exhibit unusually strong carbon and oxygen lines in their spectra. We will show that the stars are He rich with very high C and O abundances, thus, exhibiting a large fraction of helium-burning ash on their surface. They cannot be explained by any of the two mentioned evolutionary scenarios.

PG1528+025 was discovered in the Palomar-Green survey

(Green et al. 1986) as a $V = 16.4$ mag hot subdwarf and classified as sdBO. It has been observed twice within the course of the LAMOST, DR5 (Luo et al. 2019; Lei et al. 2019). These authors classified it as He-sdO and performed an automated spectral analysis using NLTE models with pure H/He composition. Luo et al. (2019) found $T_{\text{eff}} = 64\,194 \pm 593\text{ K}$, $\log g = 6.40 \pm 0.08$, and a number abundance ratio $\log \text{He}/\text{H} = 0.55 \pm 0.14$, while Lei et al. (2019) arrived at $T_{\text{eff}} = 88\,700 \pm 29\,720\text{ K}$, $\log g = 5.21 \pm 0.39$, and $\log \text{He}/\text{H} = 1.79 \pm 0.20$. PG1654+322 was also discovered in the Palomar-Green survey (Green et al. 1986) as a $V = 15.4$ mag hot subdwarf and classified as sdOC. No spectroscopic analysis was performed up to now.

2 OBSERVATIONS AND SPECTRAL ANALYSIS

We have observed PG1654+322 with the Large Binocular Telescope (LBT) on July 9, 2021, using the MODS instrument that provides two-channel grating spectroscopy. The spectra cover the wavelength region $3330\text{--}5800\text{ \AA}$ and $5500\text{--}10\,000\text{ \AA}$ with a resolving power of $R \approx 1850$ and 2300 , respectively. They are shown in Fig. 1. Besides lines of He II and weaker He I lines, we identify a plethora of carbon lines (C III and C IV) which are stronger than usual in He-sdOs. But what is most remarkable is the fact that we see rather strong oxygen lines (O III and O IV). Usually lines from this element are very weak if visible at all and can only be detected in high-resolution spectra. So just by visual inspection it is clear that these sdOs show unusually high C and O abundances. Nitrogen

* E-mail: werner@astro.uni-tuebingen.de

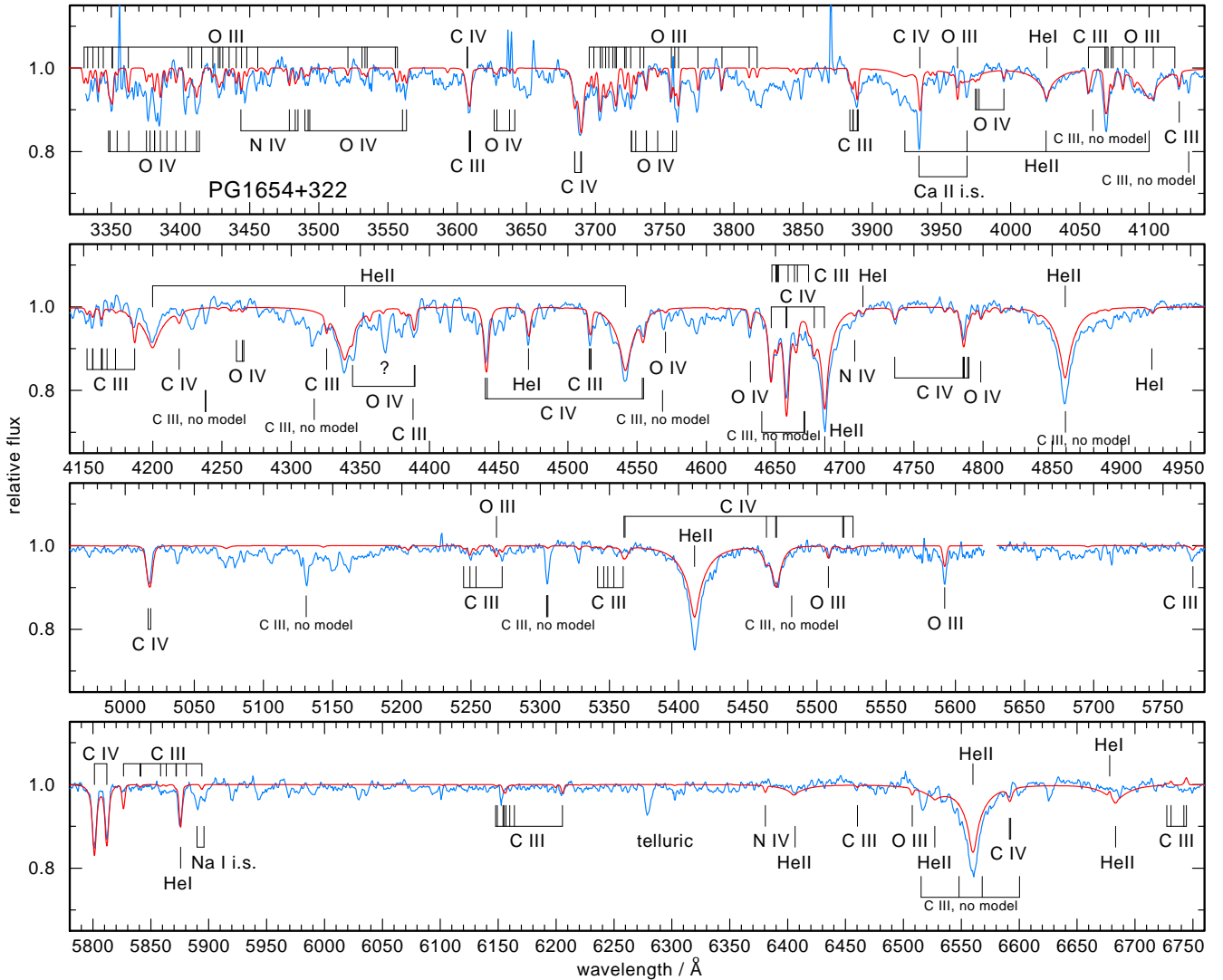


Figure 1. LBT spectrum of PG1654+322 (blue graph). Overplotted is the final model (red) with $T_{\text{eff}} = 55\,000\text{ K}$, $\log g = 5.8$, and element abundances as given in Table 1. Identified lines are labeled. Some C III lines not included in our model atom are visible in the observation and marked with “C III no model”.

lines cannot be detected and there are no hints as to the presence of hydrogen. PG1528+025 was observed in the course of the LAMOST survey (Luo et al. 2019) on March 21 and April 22, 2017. The two spectra do not show any radial velocity shift and the star is therefore likely not in a close binary system. For the spectral analysis we use the co-added spectrum. It covers the range 3700–9080 Å with $R \approx 1800$ at 5500 Å and looks very similar to PG1654+322 (Fig. 1). To search for variabilities in the light curves indicative of close binarity we checked the data archives. Both stars were observed in the course of the ZTF (Masci et al. 2019; Bellm et al. 2019) 269 and 763 times in the r-band, respectively. They do not exhibit any variability.

We used the Tübingen Model-Atmosphere Package to compute non-LTE, plane-parallel, line-blanketed atmosphere models in radiative and hydrostatic equilibrium (Werner & Dreizler 1999; Werner et al. 2003, 2012). We computed models of the type introduced in detail by Werner & Rauch (2014). They were tailored to investigate the optical spectra of relatively cool PG1159 stars. In essence, they consist of the main atmospheric constituents, namely

He, C, and O. N was included as a trace element in subsequent line-formation iterations, i.e., the atmospheric structure was kept fixed.

For the analysis of PG1654+322 we computed a small set of models with different abundances and 5000 K steps in T_{eff} and 0.3 dex steps in $\log g$. The models were calculated in a step-by-step procedure to improve the spectral fit after each single model computation. Computing a grid of models by systematically varying all parameters was prohibitive, because the model atmospheres turned out to be numerically very unstable in this parameter range.

To constrain the effective temperature we can use the ionization balances of He, C, and O. First of all, the relative strengths of lines from He I and He II are important. In particular, the neutral helium lines are very sensitive to changes in T_{eff} . In addition we can compare lines from C III and C IV, from which the C III lines react strongly on changes in temperature. Like the He I lines they become too weak at too-high temperature. In the case of oxygen, O III lines become weaker with increasing T_{eff} while O IV lines become stronger in the temperature region of interest. In the case of PG1654+322 we found a best fit at $T_{\text{eff}} = 55\,000\text{ K}$. Since models that are cooler or hotter by 5000 K predict the He I lines much too

strong or too weak, respectively, we estimate our uncertainty for the temperature determination to ± 3000 K. Constraining the surface gravity is more difficult because none of the models can fit the lower series members of the He II Pickering lines. In particular, the lines at 6560, 5412, and 4859 Å are always too weak in the models. This is reminiscent of the Balmer line problem (Bergeron et al. 1993; Werner 1996) and hence could be a hint that additional opacity sources that are not included in the models are important. So we rely on the higher series members. At too-low gravity the computed line cores become too strong while at too-high gravity the lines disappear due to pressure broadening. We find a compromise at $\log g = 5.8$ and assign a conservatively large error of ± 0.5 dex.

As to the C and O abundances, we started from helium-dominated atmosphere models with mass fractions of 0.03 for both species and gradually increased the abundances until a good by-eye fit was achieved to the spectral lines. We arrived at $C = 0.15 \pm 0.05$ and $O = 0.23 \pm 0.06$. Uncertainties were estimated from models showing too weak and too strong lines. For nitrogen, only an upper limit could be found by the absence of N IV lines in the observed spectrum. The location of the strongest N IV lines that would be detectable above an abundance threshold of $N = 0.005$ is indicated in Fig. 1. Our best fit model is computed with this value for the N abundance and some weak lines are visible. Finally we looked for an upper limit of the hydrogen abundance. Trace hydrogen would become detectable first by an emission peak of the $H\alpha$ line close to the core of the respective He II line. We found that at an abundance exceeding $H = 0.005$ this emission core would produce a noticeable dent in the He II line profile of the model which is however not observed. We therefore accept this value as an upper limit.

The best fitting model is displayed in Fig. 1. It is obvious that a number of observed lines are not present in the model. Some of them are highly excited C III lines which are not included in our model atom. These lines are indicated as “C III no model”. Many other lines remain unidentified, one of the strongest is at 4368 Å. Also, broad and shallow features are seen, for example at 3800–3850 Å, 3910–3930 Å, and 5060–5180 Å. We can only speculate that these are other high-excitation lines from C III or O III–IV. Note that some of these unidentified lines are also present in PG1528+025. We have looked for lines from other elements (Ne II, Mg II, Al III, Si III–IV, P IV–V, S IV–V, Ti V, Pb IV) discovered by Schindewolf et al. (2018), Dorsch et al. (2019), and Dorsch et al. (2021) in high-resolution spectra of He-sdOs, but to no avail.

The analysis of PG1528+025 proceeded in the same way. Its spectrum is noisier than that of PG1654+322 and it does not reach as far in the blue wavelength region (Appendix A). As a consequence, the measured element abundances have larger error estimates. PG1528+025 is cooler than PG1654+322 as can be seen by the stronger He I lines. The shape of the He II line profiles suggest a lower gravity. We determined $T_{\text{eff}} = 50\,000 \pm 3000$ K, $\log g = 5.3 \pm 0.5$, and abundances as given in Table 1. Our values for temperature and gravity are significantly lower than those found by Luo et al. (2019) mentioned in the Introduction, probably due to their model atmospheres that are composed of H and He only.

The model atmospheres for both stars were used to perform a fit to the observed spectral energy distribution (Fig. 2). Using the Fitzpatrick (1999) reddening law our synthetic spectra were reddened at the values reported by the 2D dust map of Schlafly & Finkbeiner (2011). We employed photometry from various catalogs: GALEX (Bianchi et al. 2017), Pan-STARRS1 (Chambers et al. 2016), Landolt B, V (Henden et al. 2015), Gaia DR2 and EDR3 (Gaia Collaboration et al. 2020), UKIDSS-DR9 (Lawrence et al. 2007), SDSS (Alam et al. 2015), 2MASS

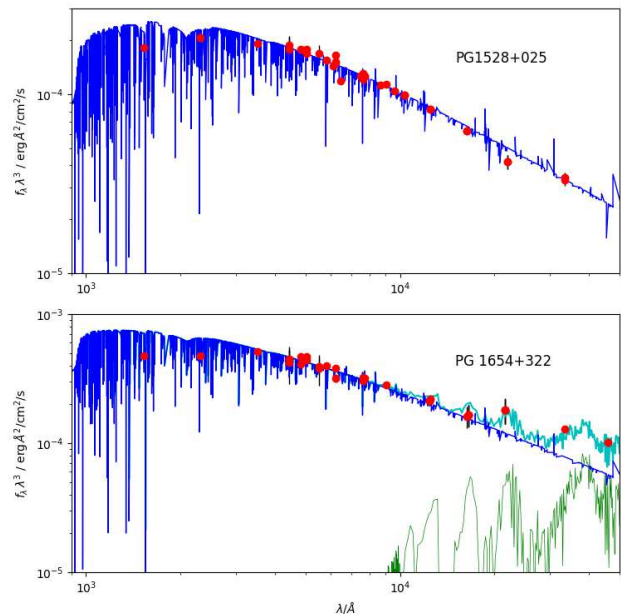


Figure 2. Comparison of our best fitting model fluxes (blue) with the observed photometry (red). The IR excess of PG1654+322 is fitted with a $T_{\text{eff}} = 2000$ K model atmosphere (see text).

(Cutri et al. 2003), and WISE (Schlafly et al. 2019). Magnitudes were converted into fluxes using the Vizier Photometry viewer (<http://vizier.unistra.fr/vizier/sed/>). The stellar radius follows from the Gaia EDR3 parallax distances from Bailer-Jones et al. (2021). The luminosity can then be computed from $L/L_{\odot} = (R/R_{\odot})^2 (T_{\text{eff}}/T_{\text{eff},\odot})^4$ (Table 1).

The visual extinction is evaluated from the standard relation $A_V = 3.1 \times E_{B-V}$ so that we obtain a dereddened visual magnitude V_0 . The spectroscopic distance d is found by the relation

$$d[\text{pc}] = 7.11 \times 10^4 \sqrt{H_{\nu} \cdot M \cdot 10^{0.4V_0 - \log g}},$$

where H_{ν} is the Eddington flux of the best-fit atmosphere model at 5400 Å (Table 1). We assume a mass of $0.8 M_{\odot}$ (see discussion below). The results are listed in Table 1 as well as the distances derived from the Gaia EDR3 parallaxes. The main error source for the spectroscopic distance is the uncertainty in the surface gravity, preventing a meaningful mass determination. Both distance determinations agree within error limits.

PG1654+322 shows an infrared excess redward of the SDSS z-band that can be reproduced with a NextGen stellar model atmosphere (Allard et al. 2012) with $T_{\text{eff}} = 2000$ K and $R = 1.7 R_{\odot}$. This radius is more than an order of magnitude higher than what is expected for an L dwarf ($\approx 0.1 R_{\odot}$). For comparison, hot Jupiters and M dwarfs in a post-common envelope binary with a central star of a planetary nebula are found to be inflated only by up to 50% (see Mol Lous & Miguel 2020; Jones et al. 2020 and references therein). A close, low-mass companion to PG1654+322 is also doubtful because at such high primary T_{eff} , typically emission lines originating from the highly irradiated side of the cool companion are visible in the optical spectra. A by-chance alignment of two such peculiar objects also seems unconvincing. Thus, PG1654+322 may harbor a gaseous disk with a similar temperature.

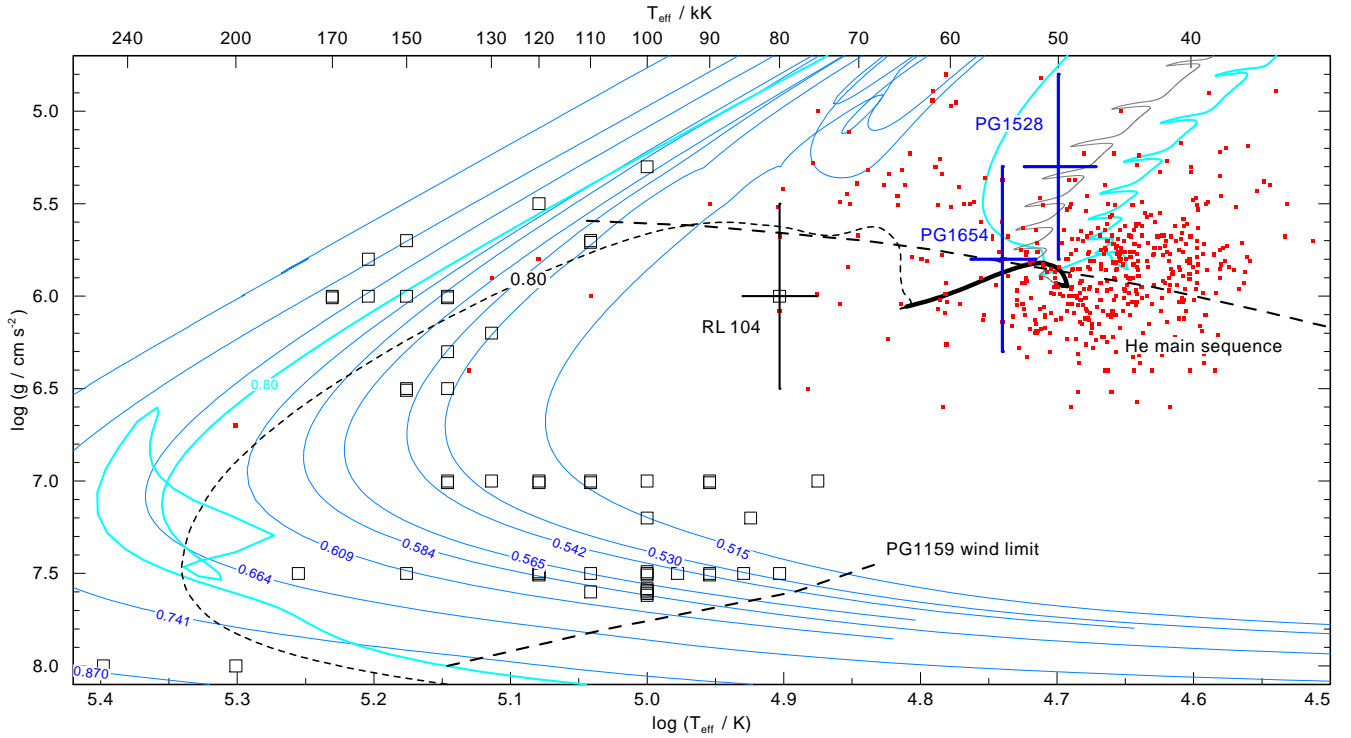


Figure 3. Position of our two CO-sdOs PG1654+322 and PG1528+025 (blue error crosses) in the $T_{\text{eff}}-\log g$ diagram among He-sdOBs (red symbols) and PG1159 stars (black symbols). Blue lines are post-AGB evolutionary tracks for late helium-flash stars (marked with remnant mass in M_{\odot}). The light blue line is track for a merger of two He-core white dwarfs with $0.8 M_{\odot}$ remnant mass ($Z = 0.02$, $\text{He} \approx 0.99$). The post-He-core burning phase of a $0.8 M_{\odot}$ remnant of a He+CO white dwarf merger ($Z = 0.001$, $\text{He} = 0.32$, $\text{C} = 0.20$, $\text{O} = 0.48$) is visualized by the thin grey line, the He-core burning phase by the thick black line, and the post-He-core burning phase by the dashed black line. The zero-age helium main sequence and the PG1159 wind limit are indicated by long-dashed lines.

Table 1. Properties of the analysed hot subdwarfs. Element abundances given in mass fractions.

	PG1654+322	PG1528+025
T_{eff}/K	$55\,000 \pm 3000$	$50\,000 \pm 3000$
$\log(g/\text{cm s}^{-2})$	5.8 ± 0.5	5.3 ± 0.5
H	< 0.005	< 0.005
He	0.62 ± 0.11	$0.58^{+0.17}_{-0.22}$
C	0.15 ± 0.05	0.25 ± 0.10
N	< 0.005	< 0.02
O	0.23 ± 0.06	$0.17^{+0.12}_{-0.07}$
L/L_{\odot}	418^{+299}_{-167}	1142^{+1960}_{-772}
R/R_{\odot}	$0.225^{+0.040}_{-0.030}$	$0.450^{+0.210}_{-0.160}$
V/mag	15.468	16.395
E_{B-V} /mag	0.025	0.043
H_{ν} /erg cm $^{-2}$ s $^{-1}$ Hz $^{-1}$	8.596×10^{-4}	7.689×10^{-4}
d /pc (spectroscopic)	2809^{+2186}_{-1229}	7059^{+5494}_{-3089}
d /pc (Gaia parallax)	3230^{+462}_{-369}	9434^{+4106}_{-3169}

3 DISCUSSION

We have analysed two helium rich ($\text{He} \approx 0.6$) hot subdwarfs which turn out to be unusually abundant in carbon ($\text{C} \approx 0.2$) and oxygen ($\text{O} \approx 0.2$; mass fractions). They establish a new spectral type that we call CO-sdOs in contrast to the usual He-sdOs which have carbon abundances from strongly subsolar to at most 3% and strongly subsolar oxygen abundances (Hirsch 2009; Németh et al. 2012; Schindewolf et al. 2018). Fig. 3 shows the position of our two

CO-sdOs in the Kiel diagram. They are within the region of He-sdOs (red symbols; Geier (2020); Jeffery et al. (2021); Luo et al. (2021)). This region is crossed by evolutionary tracks of remnants of a merger of two He-core white dwarfs. We show as two examples a $0.5 M_{\odot}$ remnant (green graph) and a $0.8 M_{\odot}$ remnant (light blue graph) from Zhang & Jeffery (2012). The He-sdOs and their CNO abundances are commonly discussed in terms of this merger scenario. However, the CO-sdOs must have another origin.

The merger of a He-core and a CO-core white dwarf was discussed in the literature since Webbink (1984). The He white dwarf is disrupted and accreted onto the CO white dwarf to form a helium giant. In a companion paper in this volume of MNRAS, Miller Bertolami et al. suggest that the CO-sdOs discovered by us are the result of such a merger but in this case the CO white dwarf was the less massive component being accreted onto the He white dwarf. This can happen only under very special conditions. First of all the first (stable) mass transfer episode has to begin close to the tip of the Red Giant Branch, producing a rather massive He-core white dwarf ($0.4 - 0.48 M_{\odot}$). The second requirement is, that the initially less massive star has to increase its mass to $1.9 - 2.1 M_{\odot}$ during this first mass transfer event, forming the lowest possible mass sdBs and CO white dwarfs with masses $0.33 - 0.4 M_{\odot}$. In Fig. 3 we present the track of a $0.8 M_{\odot}$ remnant from this scenario. It settles onto the He main sequence performing He shell flashes before central He burning starts, causing the small loops. Later on it leaves the He main sequence to become a hot white dwarf.

The position of our two CO-sdO stars in the Kiel diagram indicates that they are currently in the He-core burning stage, where CO+He white dwarf merger products spend most of their pre-white

dwarf life (≈ 22.5 Myr). The pre-He-core burning phase lasts for only 0.5 Myr, yet stars in that stage are on average ten times more luminous. Thus, for one pre-He-core burning star 4–5 He-core burning CO-sdO stars can be expected.

After He-core burning, the CO+He-merger evolves through the region of the PG1159 stars (black symbols in Fig. 3). The abundance patterns of these latter stars (approximately He = 0.30–0.85, C = 0.15–0.60, O = 0.02–0.20) are indeed found to be very similar to that of the two CO-sdOs. Usually, PG1159 stars are thought to be post-AGB (pre-) white dwarfs whose H-deficient nature was caused by a very late thermal pulse (VLTP, Werner & Herwig (2006)). In Fig. 3 VLTP evolutionary tracks from Miller Bertolami & Althaus (2006) are shown as blue graphs and the PG1159 wind limit indicating that evolution across this line transforms PG1159 stars in DA or DO white dwarfs by gravitational settling of heavy elements (Unglaub & Bues 2000). However, while a VLTP object reaches its maximum T_{eff} within $\approx 10^4$ yr, the post-He-core burning and pre-white dwarf stage ($\log g < 7.0$) of the CO+He merger lasts for 2.5 Myr. Considering that PG1159 stars in the pre-white dwarf stage are about one order of magnitude more luminous than the CO-sdOs, one could expect one luminous PG1159 star per CO-sdO in a flux limited star sample. One good candidate for this scenario is the recently discovered, low-luminosity PG1159 star RL104 (black error cross in Fig. 3, Werner et al. (2021)), whose position in the Kiel diagram is not consistent with VLTP tracks. We conclude that the CO+He white dwarf merger likely represents a non-negligible evolutionary channel creating PG1159 stars.

One may now speculate if the IR excess of PG1654+322 is a relic from a circumstellar disk formed by the disrupted CO white dwarf during the merger event. Such a disk would be made mainly of metals, and it has been suggested that it could be the birthplace of second generation planets (Livio et al. 2005). Therefore, further investigations on the nature of the IR excess of PG1654+322 are highly desirable.

DATA AVAILABILITY

Observed and computed spectra are available upon request from the corresponding author.

ACKNOWLEDGEMENTS

We thank Marcelo Miller Bertolami for informing us about his results on merger evolution calculations explaining the existence of the CO-sdOs. MP was funded by the Deutsche Forschungsgemeinschaft under grants GE2506/9-1 and GE2506/12-1. The TMAD tool (<http://astro.uni-tuebingen.de/~TMAD>) used for this paper was constructed as part of the activities of the German Astrophysical Virtual Observatory. This research has made use of NASA's Astrophysics Data System and the SIMBAD database, operated at CDS, Strasbourg, France. This research has made use of the VizieR catalogue access tool, CDS, Strasbourg, France. This work has made use of data from the European Space Agency (ESA) mission Gaia. LAMOST is operated and managed by the National Astronomical Observatories, Chinese Academy of Sciences. Based on observations obtained with the Samuel Oschin 48-inch Telescope at the Palomar Observatory as part of the Zwicky Transient Facility project, which is supported by the National Science Foundation under Grant No. AST-1440341 and the participating institutions of the ZTF collaboration. This paper used data ob-

tained with the MODS spectrographs built with funding from NSF grant AST-9987045 and the NSF Telescope System Instrumentation Program (TSIP), with additional funds from the Ohio Board of Regents and the Ohio State University Office of Research. The LBT is an international collaboration among institutions in the United States, Italy and Germany. LBT Corporation partners are: The University of Arizona on behalf of the Arizona university system; Istituto Nazionale di Astrofisica, Italy; LBT Beteiligungsgesellschaft, Germany, representing the Max-Planck Society, the Astrophysical Institute Potsdam, and Heidelberg University; The Ohio State University, and The Research Corporation, on behalf of The University of Notre Dame, University of Minnesota and University of Virginia.

References

- Alam S. et al., 2015, *ApJS*, 219, 12
 Allard F., Homeier D., Freytag B., 2012, *Philosophical Transactions of the Royal Society of London Series A*, 370, 2765
 Bailer-Jones C. A. L., Rybizki J., Fouesneau M., Demleitner M., Andrae R., 2021, *AJ*, 161, 147
 Battich T., Miller Bertolami M. M., Córscico A. H., Althaus L. G., 2018, *A&A*, 614, A136
 Bellm E. C. et al., 2019, *PASP*, 131, 018002
 Bergeron P., Wesemael F., Lamontagne R., Chayer P., 1993, *ApJ*, 407, L85
 Bianchi L., Shiao B., Thilker D., 2017, *ApJS*, 230, 24
 Chambers K. C. et al., 2016, arXiv e-prints, arXiv:1612.05560
 Cutri R. M. et al., 2003, *VizieR Online Data Catalog*, 2246, 0
 Dorsch M., Jeffery C. S., Irrgang A., Woolf V., Heber U., 2021, *A&A*, 653, A120
 Dorsch M., Latour M., Heber U., 2019, *A&A*, 630, A130
 Fitzpatrick E. L., 1999, *PASP*, 111, 63
 Gaia Collaboration, Brown A. G. A., Vallenari A., Prusti T., de Bruijne J. H. J., Babusiaux C., Biermann M., 2020, arXiv e-prints, arXiv:2012.01533
 Geier S., 2020, *A&A*, 635, A193
 Green R. F., Schmidt M., Liebert J., 1986, *ApJS*, 61, 305
 Heber U., 2016, *PASP*, 128, 082001
 Henden A. A., Levine S., Terrell D., Welch D. L., 2015, in *American Astronomical Society Meeting Abstracts*, Vol. 225, American Astronomical Society Meeting Abstracts #225, p. 336.16
 Hirsch H. A., 2009, Ph.D. thesis, Friedrich-Alexander University Erlangen-Nürnberg
 Jeffery C. S., Miszalski B., Snowdon E., 2021, *MNRAS*, 501, 623
 Jones D. et al., 2020, *A&A*, 642, A108
 Lawrence A. et al., 2007, *MNRAS*, 379, 1599
 Lei Z., Zhao J., Németh P., Zhao G., 2019, *ApJ*, 881, 135
 Livio M., Pringle J. E., Wood K., 2005, *ApJ*, 632, L37
 Luo Y., Németh P., Deng L., Han Z., 2019, *ApJ*, 881, 7
 Luo Y., Németh P., Wang K., Wang X., Han Z., 2021, *ApJS*, 256, 28
 Masci F. J. et al., 2019, *PASP*, 131, 018003
 Miller Bertolami M. M., Althaus L. G., 2006, *A&A*, 454, 845
 Mol Lous M., Miguel Y., 2020, *MNRAS*, 495, 2994
 Németh P., Kawka A., Vennes S., 2012, *MNRAS*, 427, 2180
 Schindewolf M., Németh P., Heber U., Battich T., Miller Bertolami M. M., Irrgang A., Latour M., 2018, *A&A*, 620, A36
 Schlafly E. F., Finkbeiner D. P., 2011, *ApJ*, 737, 103
 Schlafly E. F., Meisner A. M., Green G. M., 2019, *ApJS*, 240, 30
 Unglaub K., Bues I., 2000, *A&A*, 359, 1042
 Webbink R. F., 1984, *ApJ*, 277, 355
 Werner K., 1996, *ApJ*, 457, L39
 Werner K., Deetjen J. L., Dreizler S., Nagel T., Rauch T., Schuh S. L., 2003, in *Astronomical Society of the Pacific Conference Series*, Vol. 288, Hubeny I., Mihalas D., Werner K., ed, *Stellar Atmosphere Modeling*, p. 31
 Werner K., Dreizler S., 1999, *Journal of Computational and Applied Mathematics*, 109, 65

6 *K. Werner et al.*

- Werner K., Dreizler S., Rauch T., 2012, TMAP: Tübingen NLTE Model-Atmosphere Package, Astrophysics Source Code Library [record ascl:1212.015]
- Werner K., Herwig F., 2006, PASP, 118, 183
- Werner K., Rauch T., 2014, A&A, 569, A99
- Werner K., Reindl N., Dorsch M., Geier S., Munari U., Raddi R., 2021, arXiv e-prints, arXiv:2111.13549
- Zhang X., Jeffery C. S., 2012, MNRAS, 419, 452

APPENDIX A

This paper has been typeset from a \TeX/L\TeX file prepared by the author.

